- Technical Paper -

EXPERIMENTAL STUDY ON FLEXURAL BEHAVIOR OF RC BEAM RETROFITTED WITH STAINLESS STEEL REBARS AND CFRP SHEETS

Md Abul HASAN[*1], Mitsuyoshi AKIYAMA[*2], and Koya KASHIWAGI[*3]

ABSTRACT

In aggressive environments (e.g., coastal environments and de-icing salts migration), RC structure repaired with conventional methods could be corroded again since the ingress of chloride ions, water, and oxygen into the concrete will not be restrained completely. In this paper, a novel repair method for corroded RC beam using stainless steel (SS) rebars and externally bonded carbon-fiber-reinforced polymer (CFRP) sheets has been proposed and experimentally investigated. Experimental results revealed that the proposed repair method could be implemented to the deteriorated RC structures.

Keywords: stainless steel reinforcement, carbon-fiber-reinforced polymer sheet, retrofitting, reinforced concrete beam, flexural behavior

1. INTRODUCTION

In a harsh environment, reinforced concrete (RC) structure is subjected to progressive corrosion-induced deterioration, which shortens its lifetime by reducing the cross-sectional area of the rebars [1-3]. Many existing RC structures in such an environment have suffered from rebar corrosion, indicating undesired durability performance. Repair and strengthening of corroded RC members are needed to ensure structural functionality and safety, which raise their life-cycle cost (*LCC*).

In maintenance practice, corroded RC structures are typically being repaired using externally bonded steel plate or near-surface mounted reinforcement. Due to several limitations in these traditional repair methods reported in [4-5], Sidy and Jabri [6] proposed and investigated an innovative patch repair technique that considers the replacement of spalled concrete cover by a new layer and cleaning rusted bars. However, these repair operations are usually needed periodically during the structure's service life since the reoccurrence of corrosion damage could take place after repair. On the other hand, Sajedi and Huang [7] reported that when severe corrosion damage occurs in RC structures, the corroded rebars should be replaced by new rebars in the tension zone to restore flexural performance which is referred as overlaying repair approach. However, even when carbon steel (CS) rebar is used as a replacement of corroded rebar in the overlaying repair method, corrosion of the repaired beam cannot be prevented in future as the ingress of chloride ions, water, and oxygen into the concrete will not be hindered entirely [8].

Hasan et al. [9] investigated whether corrosion-resistant stainless steel (SS) rebar as a replacement of corroded rebar could be used in RC structures subjected to chloride attack. They have reported that SS rebar used in a region with higher intensity of airborne chloride hazard is cost-effective, even though the initial cost of SS rebar is substantially higher than that of CS rebar. However, it should be noted that structural performance of the repaired beam might be different from the conventional RC beam.

Substantial researches on the behavior of stainless steel structure have been reported in the literature, including the flexural behavior [10], compressive behavior [11], and the mechanical characteristic [12]. However, limited research has been conducted to investigate the structural performance of SS reinforced concrete structure, which is the main focus of the present paper. Rabi et al. [13] have performed an experimental study to investigate the flexural performance of the SS reinforced beam and proposed an analytical model for predicting flexural capacity. Nevertheless, still, there is a lack of data in the literature involving the flexural behavior of concrete beams reinforced with SS, mainly owing to SS rebar being a relatively new and novel material [13]. Moreover, these existing studies have not taken into consideration the effect of externally bonded CFRP sheets on the flexural behavior of SS reinforced beams. Therefore, more experimental studies are needed to explore the flexural performance of the SS reinforced concrete beam.

In this paper, a novel method is proposed to repair the corroded RC beam in an aggressive environment. This repair method consists of the replacement of corroded rebars with new rebars, including SS and CS rebars, and patching new concrete instead of the contaminated concrete cover followed by wrapping CFRP sheets to provide better integrity between new materials and parent concrete. An experimental plan was established to investigate the flexural performance of the RC beam retrofitted by the proposed method.

*1 Graduate School of Creative Science and Engineering, Waseda University, JCI Student Member
*2 Professor, Dept. of Civil and Environmental Engineering, Waseda University, JCI Member
*3 Graduate School of Creative Science and Engineering, Waseda University

2. EXPERIMENTAL WORK

2.1 Retrofitting method for corroded RC beams using SS rebars and CFRP sheets

In the conventional RC beam, since tensile rebars and bottom arm of stirrups are located close to the bottom surface of the beam, it is much easier to corrode owing to chloride ions ingress into the concrete through bottom surface [14]. In this research, the tensile rebars and bottom arm of the stirrups of the beams are assumed to be corroded and therefore repaired. Fig. 1 depicts a procedure for retrofitting the corroded RC beam using SS rebars and CFRP sheets, which consists of five steps. In Step 1, the contaminated concrete cover is removed in order to replace the corroded tensile reinforcements. For Step 2, the corroded bottom arm of the stirrups is trimmed, and then corroded tensile reinforcements are detached from the concrete beam. Subsequently, in Step 3, SS rebars are placed in the position of corroded tensile rebars in order to provide higher corrosion-resistance in the retrofitted beam. In Step 4, a new concrete cover is patched over the SS rebars to provide sufficient embedding for reinforcing bars, which enables them to be stressed without slipping. Lastly, in Step 5, CFRP sheets are wrapped around the cross-section of the beam to provide better integrity between parent concrete and new materials.

Since the implementation of the proposed repair method can restore the structure to its initial undamaged condition [9], the structural performance of the repaired beam is assumed to be identical with its undamaged state. In this context, twelve specimens listed in Table 1 were fabricated (i.e., without considering the substitution of damaged concrete cover by new layer) to compare the flexural behavior of CS and SS reinforced beams strengthened with CFRP sheets in order to verify the proposed retrofitting method.

2.2 Specimen's details

In order to investigate the flexural behavior of RC beam retrofitted with SS rebars and CFRP sheets, twelve specimens with 220 mm deep by 220 mm wide cross-section were fabricated listed in Table 1. All beams were 1400 mm long over 1200 mm clear span, as shown in Fig. 2, and were divided into six groups based on the tensile rebar type and stirrup configurations (Table 1). The nomenclature of the test specimens is as follows: the first and second character, C or S refers to CS or SS rebar in the 1st and 2nd layer of tensile rebar, the third character N or D refers to normal or deficient stirrup, and the following characters 0, 1, 2, and 3 refer to the strengthening scheme (0 - control beam; 1 - strengthening scheme SC_1; 2 - strengthening scheme SC_2; and 3 - strengthening scheme SC_3). The detailed drawings of the strengthening schemes (i.e., SC_1, SC_2, and SC_3) are presented in Fig. 3.

2.3 Material properties

Concrete mixture proportions are listed in Table 2. Two different types of steel bars (CS and SS) were used as tensile reinforcement. Fig. 4 presents the photo of SS rebar used in this experiment. As shown in Table 3, the yielding strength of CS rebar is 358 MPa, which is higher than that of SS rebar (334 MPa), while the ultimate strength of CS rebar (489 MPa) is remarkably lower than that of SS rebar (671 MPa). This implies that after the yielding, SS rebar shows a more significant increase in stress (i.e., strain hardening) than the CS rebar.

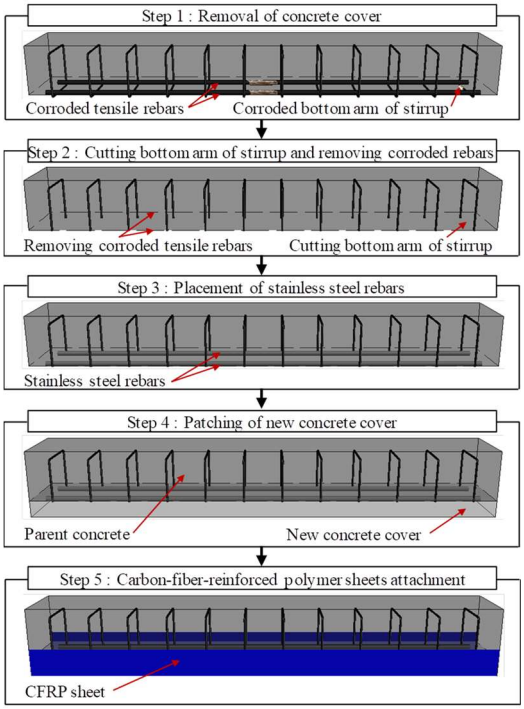

Fig. 1 Procedure of retrofitting method for corroded RC beams using SS rebars and CFRP sheets.

CFRP was used in the form of a unidirectional sheet having weight per unit area of 450 g/m^2. The tensile strength, modulus of elasticity, and elongation of CFRP sheets at fracture were found to be 3400 MPa, 245 GPa, and 1.38%, respectively.

2.4 Instrumentation and loading procedure

Fig. 2 demonstrates the layout of linear variable displacement transducer (LVDT) (i.e., D_1 and D_2) and strain gauges for concrete (i.e., CS_1 and CS_2 expressed as $CS_{1\text{-}2}$) and rebars (i.e., TS_1-TS_8 denoted as $TS_{1\text{-}8}$). Fig. 5 shows a four-point loading arrangement, which includes testing frame, hydraulic jack, LVDTs, and data acquisition system. In each stage of loading (i.e., at the occurrence of flexural cracking, δ_y, $2\delta_y$, $3\delta_y$.… where δ_y is midspan displacement at the yielding load), the cracking patterns were recorded by photographing them on two side surfaces of each beam.

3. RESULTS AND DISCUSSIONS

3.1 Effect of longitudinal rebar type on flexural performance

3.1.1 Load-deflection relationship

Load versus midspan deflection response (i.e., average deflection recorded in D_1 and D_2) curves of the control beams reinforced with CS and SS rebars (i.e., CCN-0 and SSN-0) are illustrated in Fig. 6a. The load-deflection response curves can be divided into three

Table 1 List of tested beams.

Group	Notation	Tensile reinforcement		Stirrup	Strengthening Scheme
		1st layer	2nd layer		
I	CCN-0	3ϕ16-C	2ϕ16-C	ϕ13@65-N	-
	CCN-1	3ϕ16-C	2ϕ16-C	ϕ13@65-N	SC_1
	CCN-2	3ϕ16-C	2ϕ16-C	ϕ13@65-N	SC_2
II	CCD-0	3ϕ16-C	2ϕ16-C	ϕ13@65-D	-
	CCD-2	3ϕ16-C	2ϕ16-C	ϕ13@65-D	SC_2
III	SCN-2	3ϕ16-S	2ϕ16-C	ϕ13@65-N	SC_2
IV	SCD-2	3ϕ16-S	2ϕ16-C	ϕ13@65-D	SC_2
V	SSN-0	3ϕ16-S	2ϕ16-S	ϕ13@65-N	-
	SSN-1	3ϕ16-S	2ϕ16-S	ϕ13@65-N	SC_1
	SSN-3	3ϕ16-S	2ϕ16-S	ϕ13@65-N	SC_3
VI	SSD-0	3ϕ16-S	2ϕ16-S	ϕ13@65-D	-
	SSD-2	3ϕ16-S	2ϕ16-S	ϕ13@65-D	SC_2

Note: C = carbon steel; S = stainless steel; N = normal stirrup; D = deficient (i.e., without bottom arm) stirrup; ϕ = diameter of rebar; 0 = "-" = control beam; 1 = strengthening scheme SC_1; 2 = strengthening scheme SC_2; and 3 = strengthening scheme SC_3.

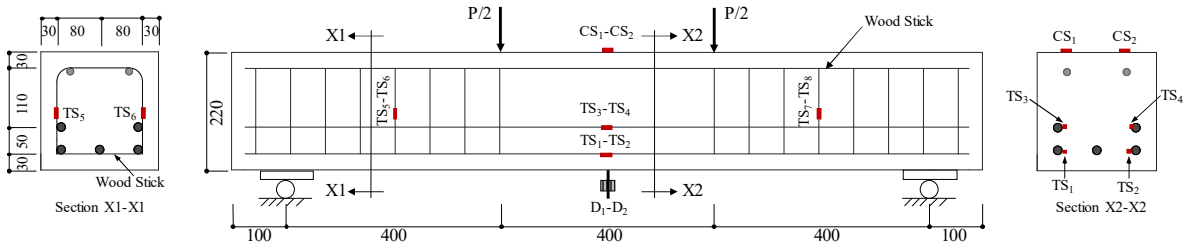

CS_1-CS_2 (CS_{1-2}) = Strain gauges attached on concrete; TS_1-TS_8 (TS_{1-8}) = Strain gauges attached on rebars; and D_1-D_2 = LVDTs attached to measure the midspan deflection.

Fig. 2 Strain gauges on concrete and rebars in the tested beam (all dimensions are in mm).

different stages, as presented in Fig. 6a. In the first stage, CCN-0 and SSN-0 are uncracked, and thus they have the same stiffness prior to cracking due to the same sectional moment of inertia. In the second stage, flexural cracks start to develop, which leads to a decrease in the flexural stiffness for both beams. CCN-0 has larger post-cracking stiffness than SSN-0.

In the third stage, flexural-shear cracks started to develop outside the constant-moment region, and typical flexural failure mode was observed for two beams, by yielding of the steel reinforcement followed by concrete crushing in the vicinity of the beam's midspan. For CCN-0, after concrete crushing, the aluminum angle to measure the deflection of the beams did not perform well which results in the vertical movement independent of the load. This led to a load drop (see Fig. 6a). The failure mode of the beams can also be verified by analyzing the load-strain relationship of the constituent materials, as shown in Figs. 6b and 6c. At the maximum load, strain in concrete (see Fig. 6b) and tensile rebar (see Fig. 6c) are significantly higher than their ultimate (i.e., ε_{cu} = 0.0035) and yielding strain, respectively, while strain of stirrup is found to be substantially lower than its yielding strain. The load-strain data of the beams support the observed flexural failure mode shown in Fig. 7. CCN-0 displayed a significant increase in yielding and maximum load over the SSN-0 (Fig. 6 and Table 4). Moreover, there was no sudden loss in stiffness for two beams, which reveals the evidence of excellent bond characteristics of the SS rebars used in this study.

3.1.2 Cracking behavior

The measurements on cracks of the control beams reinforced with CS and SS rebars at the yielding load are

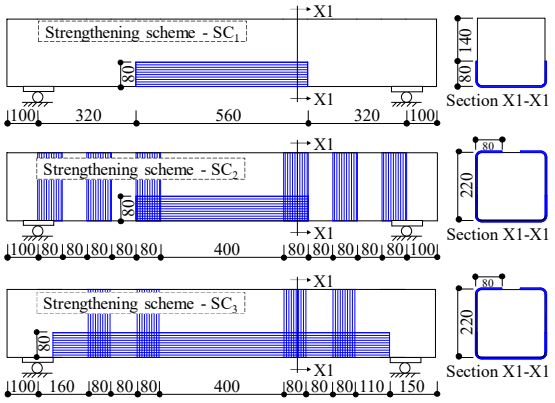

Fig. 3 Drawings of strengthening schemes.

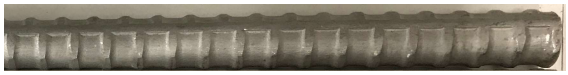

Fig. 4 Photo of stainless steel rebar.

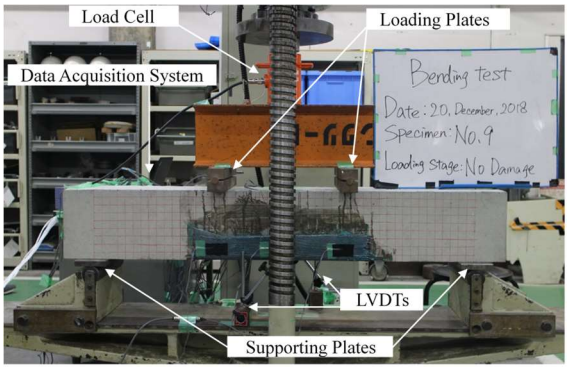

Fig. 5 Four-point testing setup.

Table 2 Concrete mixing proportion.

Constituent	Unit	Quantity
Ordinary Portland cement [a]	kg/m^3	359
Fine sand [b]	kg/m^3	757
20 mm crushed aggregate [c]	kg/m^3	972
Total free water	l/m^3	177
Admixture-Pozzolith 390N [d]	l/m^3	1.795
Air content (%)	%	5
Temperature	^{0}C	25

[a] Normal type-I Portland cement with a specific density of 3.16 g/cm^3; [b] Fine aggregate with a specific density of 2.60 g/cm^3 and a fineness modulus of 2.64; [c] Coarse aggregate (G_{max} < 20 mm) with a specific density of 2.64 g/cm^3; and [d] Air-entraining agent.

Table 3 Material properties of rebar.

Property	Carbon steel		Stainless steel
Diameter (mm)	16	13	16
f_y [a] (MPa)	358	360	334
f_u [b] (MPa)	489	516	671
E [c] (GPa)	200	200	197
η [d] (%)	28	23	52

[a] Yield strength of the steel bar; [b] Ultimate strength; [c] Modulus of elasticity; and [d] Ultimate elongation (%).

Table 4 Test results.

Notation of specimen	Yielding load			Maximum load (kN)
	P_y [a] (kN)	w_{cr} [b] (mm)	Crack number	
CCN-0	2.09×10^2	0.20	11	2.96×10^2
CCN-1	2.23×10^2	0.65	4	2.80×10^2
CCN-2	2.16×10^2	0.50	4	2.94×10^2
CCD-0	1.89×10^2	0.20	13	2.84×10^2
CCD-2	2.08×10^2	0.35	4	2.95×10^2
SCN-2	1.84×10^2	0.20	3	2.61×10^2
SCD-2	2.10×10^2	0.20	2	2.99×10^2
SSN-0	1.72×10^2	0.20	9	2.74×10^2
SSN-1	2.08×10^2	0.25	5	2.73×10^2
SSN-3	2.05×10^2	0.03	1	3.12×10^2
SSD-0	1.74×10^2	0.30	10	2.68×10^2
SSD-2	2.10×10^2	0.15	3	2.93×10^2

[a] Yielding load; and [b] Crack width at rebar yielding.

shown in Table 4. It can be seen that the number of cracks appeared to be marginally higher for CCN-0 over SSN-0, even though they provide a similar crack width at the yielding load. Moreover, as shown in Fig. 7, there had no noticeable difference in the crack patterns obtained for CCN-0 and SSN-0. These findings exhibited that the effect of tensile rebar type (i.e., CS versus SS) on the cracking behavior of RC beams are insignificant.

3.2 Effect of deficient stirrup on flexural performance

3.2.1 Load-deflection relationship

To examine the effect of stirrup configuration on the flexural behavior of RC beams, SSN-0 and SSD-0 are considered. Fig. 8a shows load versus midspan deflection responses of the considered beams, which indicates the pre-cracking stiffness of the beams with normal and deficient stirrups are approximately identical. Between the occurrence of flexural cracking and yielding of steel, stiffness of the beams with normal and deficient stirrups was also identical since similar tensile reinforcement types were used in both beams. After yielding of the tension steel, the specimens continued to carry the increasing load, and the maximum load on these beams was observed at the crushing of concrete at midspan. The maximum load of the RC beam with normal and deficient stirrups are approximately identical (see Fig. 8a and Table 4). The load-strain relationship of the concrete and tensile rebar shown in Figs. 8b and 8c confirm the flexural failure. It should be noted that as the strain gauges were damaged at a certain load level, the complete load-strain curves are not provided.

3.2.2 Cracking behavior

Fig. 7 shows the crack patterns of SSN-0 and SSD-0 at the maximum load. No significant difference in crack spacing, the number of cracks, and the crack patterns were observed between the beam with normal and deficient stirrups. However, higher crack width was measured for the beam with deficient stirrups than that of normal stirrups. For example, at yielding load, the maximum crack width for SSD-0 and SSN-0 are 0.30 mm and 0.20 mm, respectively, as shown in Table 4. This implies that in SSN-0, relatively superior bond performance is exhibited than the SSD-0, which could be due to the difference in the confinement effect induced by normal and deficient stirrups.

3.3 Effect of CFRP sheet wrapping on flexural performance of RC beam with SS and CS rebars

3.3.1 Load-deflection relationship

The load-deflection behavior of CS and SS reinforced beams strengthened with SC_1 and SC_2 are depicted in Figs. 9a and 9b, respectively. As shown in Fig. 9a, CCN-1 and SSN-1 exhibited linear behavior up to the initial cracking load, beyond which marginal change in the slope of load-deflection curves was observed. By further increasing the load, the yielding of the internal steel reinforcement occurred in the SSN-1 and CCN-1. The post-cracking stiffness of CCN-1 was found higher than the SSN-1. After the yielding, two beams continued to carry the increasing load, and the occurrence of concrete cover separation was observed at the end of the CFRP sheet wrapping due to the stress concentration. The maximum load of CCN-1 and SSN-1 was recorded at the concrete crushing. Compared to SSN-1, CCN-1 shows a marginally higher maximum load, and a gradually decreasing trend is noticed for two beams beyond the maximum load.

On the other hand, Fig. 9b shows that load-deflection behavior of CS and SS reinforced beams with SC_2 strengthening scheme (i.e., CCD-2, SCD-2, and SSD-2) are approximately similar. However, as expected, the yielding load of CCD-2 is marginally higher than the SCD-2 and SSD-2 owing to the higher yielding strength of CS rebar over the SS. After the yielding of rebar, three beams continued to carry the increasing load; however, the concrete cover separation was observed for these beams, even though U-wraps anchorage was provided at the ends of the bending region on the continuous surface bonded U-wraps. Since U-wrap anchorage was debonded in CCD-2, the load-carrying capacity of this

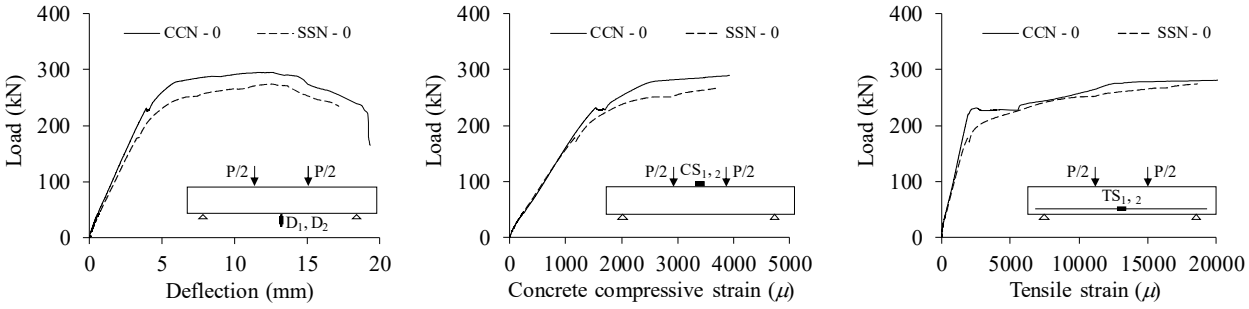

Fig. 6 (a) load-deflection (b) load-concrete strain, and (c) load-rebar strain relationships of CCN-0 and SSN-0.

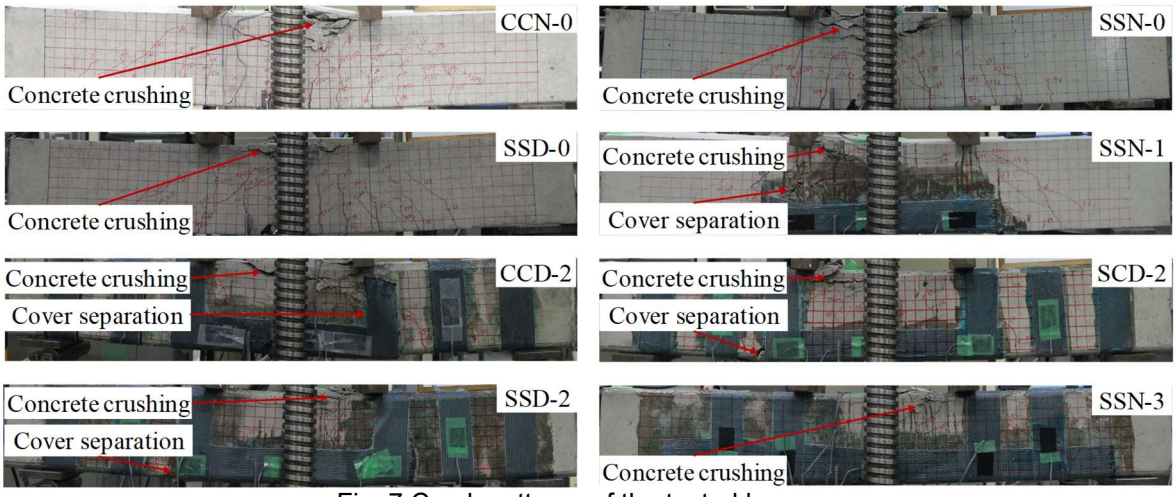

Fig. 7 Crack patterns of the tested beams.

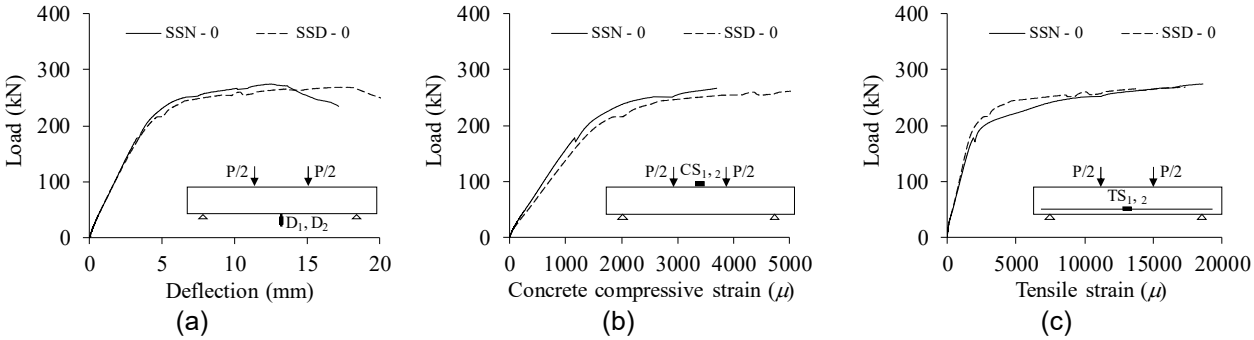

Fig. 8 (a) load-deflection (b) load-concrete strain, and (c) load-rebar strain relationships of SSN-0 and SSD-0.

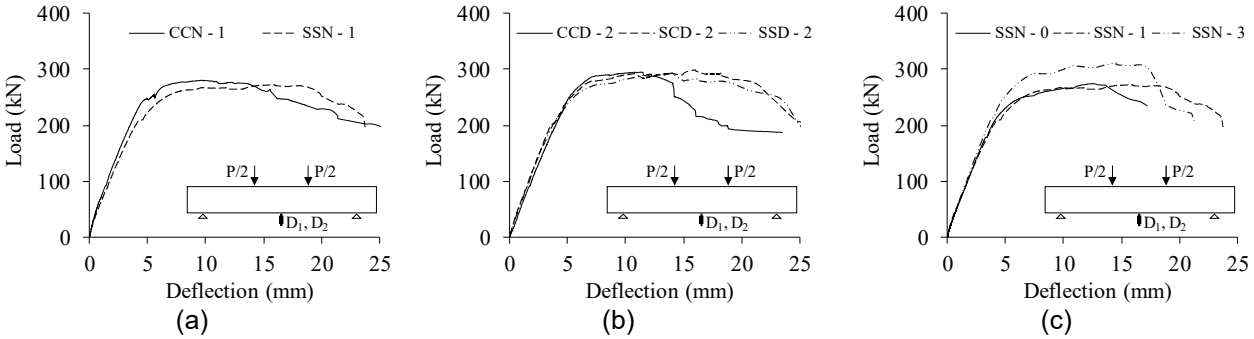

Fig. 9 Effect of strengthening scheme (a) SC_1, (b) SC_2, and (c) SC_3 on load-deflection relationships of beams.

specimen abruptly decreased.

When strengthening scheme SC_3 is considered, the structural performance is enhanced remarkably compared to the control (SSN-0) and SC_1 strengthened beam (SSN-1), as shown in Fig. 9c. Since aluminum angles were detached due to concrete crushing, the complete load-deflection curve of SSN-3 is not provided. The yielding and maximum loads for SSN-3 are increased by 19.50% and 13.87% (see Table 4 and Fig. 9c) than the control beam, as the CFRP sheets in SC_3

contribute in carrying load due to presence of sufficient anchorage length. Moreover, the SC_3 strengthening scheme could prevent the concrete cover separation, and typical flexural failure mode was observed for SSN-3, by yielding of steel reinforcement followed by concrete crushing, as shown in Fig. 7.

3.3.2 Cracking behavior

Table 4 shows that the number of cracks of the RC beam strengthened using SC_1 (i.e., CCN-1 and SSN-1) are approximately identical at the yielding load. However, CCN-1 and SSN-1 have larger crack widths compared to control beams (i.e., CCN-0 and SSN-0) at the yielding load. The crack having maximum width of these beams was located at the end of CFRP sheet wrapping, where concrete cover separation occurred. This implies that in the RC beam strengthened with CFRP sheet, the maximum crack width is dominated by the severity of the stress concentration at the end of the CFRP sheet wrapping, leading to concrete cover separation.

On the other hand, the RC beam strengthened using SC_2 (e.g., CCD-2, SCD-2, and SSD-2) presents fewer cracks than the control beam and the beams strengthened using SC_1 at the yielding and maximum loads. In addition, at the yielding load, the maximum crack widths of CCD-2, SCD-2, and SSD-2 were measured as 0.35 mm, 0.20 mm, and 0.15 mm, respectively, which are lower than that of beam (e.g., CCN-1) strengthened using SC_1. The reason behind the smaller crack width for CCD-2, SCD-2, and SSD-2 could be due to the presence of anchorage at the end of continuous wrapped CFRP sheets. For SSN-3, the lowest number of cracks were occurred, and crack widths were reduced compared to the remaining test specimens at the yielding and maximum loads, as shown in Fig. 7 and Table 4.

4. CONCLUSIONS

(1) A novel repair technique using SS rebars and CFRP sheet has been proposed for the corroded RC beam.
(2) The experimental results of CS and SS reinforced beams demonstrate that the longitudinal rebar type with identical physical and mechanical properties does not influence the structural performance and failure mode significantly, which confirms that the existing deteriorated RC structures can be repaired with higher corrosion-resistant SS rebars.
(3) The maximum loads of the RC beams with normal and deficient stirrups are almost the same. However, if the ratio of shear to flexural strength of the RC beam is close to 1.0, cutting the bottom arm of stirrup may affect the failure mode. Therefore, further research is needed to investigate the structural behavior of shear critical beam.
(4) Since the effectiveness of CFRP sheet wrapping schemes on the flexural performance of CS and SS reinforced beams are identical, the similar CFRP sheet wrapping schemes for ordinary RC beams can be applied to SS reinforced beams.

REFERENCES

[1] Akiyama, M., Frangopol, D. M., and Yoshida, I., "Time-dependent reliability analysis of existing RC structures in a marine environment using hazard associated with airborne chlorides," Engineering Structures, Vol. 32, Nov. 2010, pp. 3768-3779.

[2] Hasan, M. A., Yan, K., Qi, S., and Akiyama, M., "Effect of rebar types on the life-cycle cost of RC structures in a marine environment," Proceeding of Japan Concrete Institute, Vol. 40, July 2018, pp. 1393-1398.

[3] Akiyama, M., Frangopol, D. M., and Suzuki, M., "Integration of the effects of airborne chlorides into reliability-based durability design of reinforced concrete structures in a marine environment," Structure and Infrastructure Engineering, Vol. 8, Feb. 2012, pp. 125-134.

[4] Jones, R., Swamy, R. N., and Charif, A., "Plate separation and anchorages of reinforced concrete beams strengthened by epoxy-bonded steel plates," Structural Engineer, Vol. 66, Mar. 1988, pp. 85-94.

[5] Kreit, A., Al-Mahmoud, F., Castel, A., and Francois, R., "Repairing corroded RC beam with near-surface mounted CFRP rods," Materials and Structures, Vol. 44, Aug. 2011, pp. 1205-1217.

[6] Al-Saidy, A. H., and Al-Jabri, K. S., "Effect of damaged concrete cover on the behavior of corroded concrete beams repaired with CFRP sheets," Composite Structures, Vol. 93, June 2011, pp. 1775-1786.

[7] Sajedi, S., and Huang, Q., "Reliability-based life-cycle-cost comparison of different corrosion management strategies," Engineering Structures, Vol. 186, May 2019, pp. 52-63.

[8] Kobayashi, K., and Rokugo, K., "Mechanical performance of corroded RC member repaired by HPFRCC patching," Construction and Building Materials, Vol. 39, Feb. 2013, pp. 139-147.

[9] Hasan, M. A., Yan, K., Lim, S., Akiyama, M., and Frangopol, D. M., "LCC-based identification of geographical locations suitable for using stainless steel rebars in RC girder bridges," Structure and Infrastructure Engineering, 2019 (in press).

[10] Huang, Y., and Young, B., "Design of cold-formed lean duplex stainless steel members in combined compression and bending," Journal of Structural Engineering, ASCE, Vol. 141, May 2015, pp. 1-10.

[11] Afshan, S., and Gardner, L., "The continuous strength method for structural stainless steel design," Thin-Walled Structures, Vol. 68, July 2013, pp. 42-49.

[12] Ramussen, K. J. R., "Full-range stress-strain curves for stainless steel alloys," Journal of Constructional Steel Research, Vol. 59, Jan. 2003, pp. 47-61.

[13] Rabi, M., Cashel, K. A., and Shamass, R., "Flexural analysis and design of stainless steel reinforced concrete beams," Engineering Structures, Vol. 198, Nov. 2019, pp. 1-13.

[14] Ullah, R., "Mechanical behavior of reinforced concrete beams with locally corroded shear reinforcement," Doctoral thesis, Hokkaido University, Sapporo, Hokkaido, Sep. 2017, pp. 1-82.